Innovation, Sciences et Développement économique Canada
Office de la Propriété Intellectuelle du Canada

Innovation, Science and Economic Development Canada
Canadian Intellectual Property Office

CA 3081608 C 2023/09/05

(11)(21) **3 081 608**

(12) **BREVET CANADIEN**
CANADIAN PATENT

(13) **C**

(22) **Date de dépôt/Filing Date:** 2020/06/01

(41) **Mise à la disp. pub./Open to Public Insp.:** 2020/09/11

(45) **Date de délivrance/Issue Date:** 2023/09/05

(30) **Priorité/Priority:** 2020/02/28 (KR10-2020-0024795)

(51) **Cl.Int./Int.Cl.** ***G05D 1/10*** (2006.01), ***B64C 19/00*** (2006.01), ***G05B 13/04*** (2006.01)

(72) **Inventeur/Inventor:**
AHN, SEOUNG GYU, KR

(73) **Propriétaire/Owner:**
PABLO AIR CO., LTD., KR

(74) **Agent:** AVENTUM IP LAW LLP

(54) **Titre : PROCEDE D`EVITEMENT DE COLLISION D`UN VEHICULE AERIEN SANS PILOTE**
(54) **Title: METHOD OF AVOIDING COLLISION OF UNMANNED AERIAL VEHICLE**

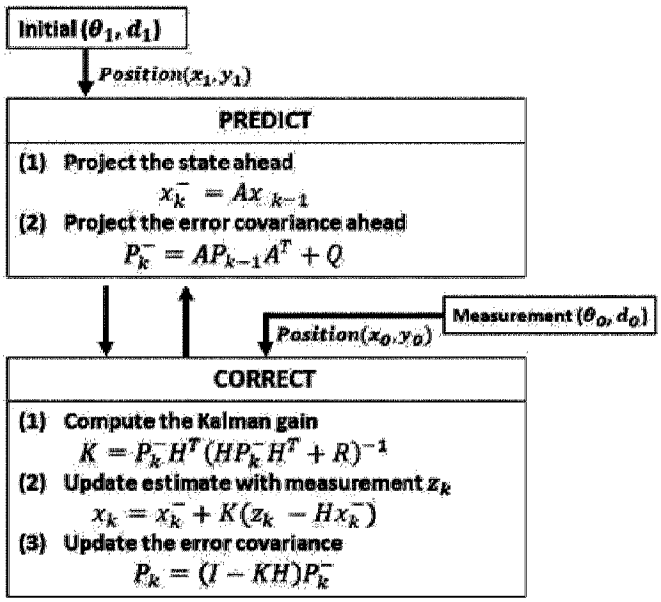

(57) **Abrégé/Abstract:**
Provided is a method of avoiding collision of an unmanned aerial vehicle with an obstacle, the method including: calculating two potential fields using current positional information of the unmanned aerial vehicle, a target point that is set, and positional information of the obstacle measured by a sensor; computing an attractive force and a repulsive force by differentiating the computed potential fields, respectively; computing a direction of a potential force that results from adding up the computed attractive force and repulsive force; and performing control that brings about a change from the computed direction of the potential force to a direction in which the unmanned aerial vehicle moves.

ABSTRACT

Provided is a method of avoiding collision of an unmanned aerial vehicle with an obstacle, the method including: calculating two potential fields using current positional information of the unmanned aerial vehicle, a target point that is set, and positional information of the obstacle measured by a sensor; computing an attractive force and a repulsive force by differentiating the computed potential fields, respectively; computing a direction of a potential force that results from adding up the computed attractive force and repulsive force; and performing control that brings about a change from the computed direction of the potential force to a direction in which the unmanned aerial vehicle moves.

Date Reçue/Date Received 2020-06-01

METHOD OF AVOIDING COLLISION OF UNMANNED AERIAL VEHICLE

BACKGROUND OF THE INVENTION

Field of the Invention

The present invention relates to a method of avoiding collision of an unmanned aerial vehicle and more particularly, to a method of avoiding collision of an unmanned aerial vehicle on the basis of a potential field taking into consideration a relative velocity of an obstacle.

Description of the Related Art

When damaged due to collision in the air, an unmanned aerial vehicle is highly likely to fall to the ground. In such a case, there is a high risk of causing losses of both life and property or a forest fire. Particularly, a collision in a downtown area is highly likely to cause a loss of life. Thus, it is necessary to prevent unexpected collision. In addition, with the development of the industry related to unmanned aerial vehicles, there is an increasing concern with collision avoidance. Accordingly, research has been made on sensors and algorithms for collision avoidance.

Devices for recognizing and avoiding collision of the unmanned aerial vehicle are broadly categorized into

Date Reçue/Date Received 2020-06-01

collaborative sensors that exchange pieces of data by communicating with a counterpart aircraft using transponders such as a traffic collision avoidance system (TCAS) and automatic dependent surveillance broadcast (ADSB), and non-collaborative sensors, such as a radar, an image sensor, and LiDAR, that obtain information by making a measurement. The cooperative sensor is a sensor that transmits and receives pieces of information, such as a position, altitude, and velocity of the obstacle. The cooperative sensor is unsuitable for avoiding collision with an expected obstacle or a terrain feature because a primary objective thereof is to avoid collision between unmanned aerial vehicles or collision with a manned aerial vehicle. On the other hand, the non-collaborative sensor can recognize an obstacle on the basis of information measured by a sensor and can detect collision with the obstacle and avoid the collision therewith. Thus, it is possible not only to avoid a terrain feature, but also to avoid collision with an expected obstacle.

Algorithms that are applicable to existing unmanned aerial vehicles include a collision avoidance algorithm based on a potential field technique, a collision avoidance algorithm using geometric information, a collision avoidance algorithm using a bearing angle, a collision avoidance algorithm using an optical flow, and so on.

The collision avoidance algorithm using the bearing angle,

Date Reçue/Date Received 2020-06-01

which is an algorithm for avoiding collision by keeping an obstacle at a safe position in the field of view of an image sensor, may be difficult to utilize in a situation where various obstacles are recognized by the image sensor. The collision avoidance algorithm using the optical flow, which is also an algorithm for avoidance through computation of the optical flow, may be difficult to utilize in a downtown area where obstacles are omnidirectionally recognized. The collision avoidance algorithm based on the potential field technique is an algorithm for avoiding collision with a force that is obtained by adding up an attractive force and a repulsive force that are generated by utilizing information of an obstacle obtained by a sensor. For this reason, it is determined that the collision avoidance algorithm based on the potential field technique is suitable for collision avoidance in a complex situation. However, a general potential field results from considering only a distance to an obstacle, and thus has poor performance in terms of avoiding a moving obstacle. In this manner, an existing collision avoidance algorithm is not designed as a result of considering characteristics of a downtown area where high-rising buildings are highly packed together and where an unexpected situation is highly likely to occur. Thus, it is necessary to discuss whether it is possible to utilize an existing algorithm in the downtown area.

Date Reçue/Date Received 2020-06-01

Examples of the related art include Korean Unexamined Patent Application Publication No. 2019-0004176 titled "APPARATUS AND METHOD FOR AVOIDING COLLISION OF UNMANNED AERIAL VEHICLE WITH OBSTACLE" and Korean Patent No. 10-1501528 titled "SYSTEM AND METHOD FOR PREVENTING COLLISION OF UNMANNED AERIAL VEHICLE."

SUMMARY OF THE INVENTION

An objective of the present invention is to provide an algorithm which prevents collision in an area where obstacles are highly packed together.

Another objective of the present invention is to provide an algorithm which prevents collision when any object other than a specific object has the risk of collision.

Still another objective of the present invention is to provide an algorithm which presents collision not only in an expected situation, but also in a situation that is difficult to predict.

Still another objective of the present invention is to provide an algorithm which prevents collision not only with a stationary obstacle, but also with a moving obstacle.

Still another objective of the present invention is to provide an obstacle detection sensor that is capable of being mounted on an unmanned aerial vehicle.

Date Reçue/Date Received 2020-06-01

According to an aspect of the present invention, there is provided a method of avoiding collision of an unmanned aerial vehicle with an obstacle, the method including: calculating two potential fields using current positional information of the unmanned aerial vehicle, a target point that is set, and positional information of the obstacle measured by a sensor; computing an attractive force and a repulsive force by differentiating the computed potential fields, respectively; computing a direction of a potential force that results from adding up the computed attractive force and repulsive force; and performing control that brings about a change from the computed direction of the potential force to a direction in which the unmanned aerial vehicle moves.

With a method of avoiding collision of an unmanned aerial vehicle according to the present invention, an algorithm which prevents collision in an area where obstacles are highly packed together, and thus the unmanned aerial vehicle can be prevented from colliding an obstacle. In addition, according to the present invention, a collision avoidance algorithm which prevents collision with a moving obstacle, as well as with a stationary obstacle, is avoidable is provided. This provides the advantage that collision is also avoidable in a situation that is difficult to predict.

In addition, according to the present invention, LiDAR is used as an obstacle detection sensor that senses an obstacle.

Date Reçue/Date Received 2020-06-01

This provides performance that is higher than is the case with any other sensor.

According to one aspect of the invention, there is provided method of avoiding collision of an unmanned aerial vehicle with an obstacle, the method comprising:

calculating two potential fields using current positional information of the unmanned aerial vehicle, a target point that is set, and positional information of the obstacle measured by a sensor;

computing an attractive force and a repulsive force by differentiating the computed potential fields, respectively;

computing a direction of a potential force that results from adding up the computed attractive force and repulsive force; and

performing control that brings about a change from the computed direction of the potential force to a direction in which the unmanned aerial vehicle moves;

wherein the step of computing of the potential field includes an attractive potential field that is computed with the current positional information of the unmanned aerial vehicle and the target point that is set, and a repulsive potential field that is computed with the current positional information of the unmanned aerial vehicle and a positional information of the obstacle,

the repulsive potential field is proportional to a coefficient of the repulsive force that is a set coefficient,

a change in the position of the unmanned aerial vehicle for a set time is computed,

the coefficient of the repulsive force is reduced in a case where the computed change in the position of the unmanned aerial vehicle is smaller than a setting value, and

Date Reçue/Date Received 2022-10-05

the case where the computed change in the position of the unmanned aerial vehicle is smaller than the setting value for the given time is a case where the target point is positioned within a range where the obstacle exerts an influence and the repulsive force that is generated by the obstacle is greater than the attractive force that is generated by the target point.

BRIEF DESCRIPTION OF THE DRAWINGS

FIGS. 1A and 1B are respectively a block diagram and a table that show an algorithm of a Kalman filter and constituent elements of the Kalman filter according to the present invention;

FIG. 2 is a graph comparing an actual value and a measurement value for a path along which an obstacle moves and a result obtained by applying the Kalman filter;

FIG. 3 is a graph comparing an actual velocity of an obstacle and a velocity that is estimated with the Kalman filter;

FIG. 4 is a graph showing a difference between the actual velocity of the obstacle and the velocity that is estimated with the Kalman filter;

FIG. 5 is a graph comparing the actual value and the measurement value for the path along which the obstacle moves and a result for the Kalman filter;

FIG. 6 is a graph comparing the actual velocity of the obstacle and the velocity that is estimated with the Kalman filter;

FIG. 7 is a graph showing the difference between the

Date Reçue/Date Received 2022-10-05

actual velocity of the obstacle and the velocity that is estimated with the Kalman filter;

FIG. 8 is a graph illustrating a velocity estimation RMSE in terms of LiDAR accuracy;

FIG. 9 is a graph illustrating a velocity estimation RMSE in terms of LiDAR resolution;

FIG. 10 is a graph illustrating attractive potential field parameters;

FIG. 11 is a graph illustrating an example of an attractive potential field;

FIG. 12 is a graph illustrating an example of an attractive potential field contour;

FIG. 13 is a graph illustrating repulsive potential field parameters;

FIG. 14 is a graph illustrating an example of a repulsive potential field;

FIG. 15 is a graph illustrating an example of a repulsive potential field contour;

FIG. 16 is a diagram illustrating the first local minima;

FIG. 17 is a diagram illustrating the second local minima;

FIG. 18 is a diagram illustrating the third local minima;

FIG. 19 is a flowchart illustrating a local minima algorithm; and

FIG. 20 is a diagram illustrating a collision avoidance algorithm.

Date Reçue/Date Received 2020-06-01

DETAILED DESCRIPTION OF THE INVENTION

The above-described aspects of the present invention and additional aspects thereof will be apparent from a preferable embodiment that will be described with reference to the accompanying drawings. Descriptions will be provided below so in sufficient detail that a person of ordinary skill in the art clearly can understand and implement the embodiment of the present invention.

A potential field generates a repulsive force against an obstacle and thus achieves avoidance. Because of this, an algorithm is not complicated, and computation is simple. Thus, collision is sufficiently avoidable in a downtown area where obstacles are tightly packed together. A collision avoidance algorithm based on the potential field generates the potential field with respect to a surrounding situation. The avoidance is achieved on the basis of the generated potential field. Because of this, the collision is avoidable in a manner that is suitable for the surrounding situation.

According to the present invention, as an obstacle detection sensor, LiDAR which can recognize a specific object and can be mounted in an unmanned aerial vehicle is used.

A general potential field is given as a function of a distance to an obstacle, and thus has poor performance in

Date Reçue/Date Received 2020-06-01

avoiding a moving obstacle. According to the present invention, a velocity relative to the obstacle is taken into consideration when generating the potential field. Thus, the performance in avoiding the moving obstacle is improved.

In addition, according to the present invention, in order to compensate for a disadvantage of the general potential field, the potential field is generated considering the velocity relative to the obstacle. Furthermore, performance of a proposed collision avoidance algorithm is verified through modeling and simulation of an urban environment, and an analysis is made in comparison with an existing potential field.

The collision avoidance algorithms according to the present invention are broadly divided into three parts. First, various obstacles, such as buildings in a downtown area and other unmanned aerial vehicles including an intruding unmanned aerial vehicle, are detected, and a potential collision with the detected obstacle is recognized. According to the present invention, LiDAR that is used as a detection sensor detects an obstacle. Obstacle detection that uses LiDAR omnidirectionally detects an obstacle using Radar-LiDAR, and, when the detected object comes within a fixed range, determines it as an obstacle. Second, in a case where a potential collision of the unmanned aerial vehicle is recognized, a collision avoidance direction is determined, taking into consideration a distance

Date Reçue/Date Received 2020-06-01

between the unmanned aerial vehicle and the obstacle, a direction and velocity of the obstacle, and a velocity of the unmanned aerial vehicle. The collision avoidance algorithm according to the present invention determines a direction in which the unmanned aerial vehicle can avoid collision. Last, the unmanned aerial vehicle moves in the direction of avoiding a collision. While avoiding the collision in a downtown area, the unmanned aerial vehicle may experience a local minima phenomenon where an unmanned aerial vehicle flies repeatedly within a fixed section. According to the present invention, when determined as experiencing the local minima phenomenon, the unmanned aerial vehicle can overcome the local minima phenomenon by adjusting a potential gain.

Obstacle detection sensors for avoiding the collision of the unmanned aerial vehicle are broadly categorized into collaborative sensors that exchange pieces of data on an obstacle by communicating with a counterpart aircraft and a control system using transponders such as TCAS and ADSB, and non-collaborative sensors, such as an image sensor, a radar, and LiDAR, that determine an obstacle using measurement information.

LiDAR can acquire information on a distance to a detection target in a 2D or 3D coordinate frame while a laser-based module rotates. According to a method of modulating a laser signal, LiDAR comes in two types: a time-of-flight (TOF) type

Date Reçue/Date Received 2020-06-01

and a phase-shift type. According to the present invention, as illustrated above, among non-collaborative sensors, LiDAR that can measure the distance to the obstacle and the direction thereof is utilized as a sensor for determining the obstacle.

Particularly, in measuring the distance to the obstacle, LiDAR according to the present invention is capable of making a measurement by a total of 30° at intervals of 2° using a total of 16 channels, with respect to the vertical axis, and is capable of making a measurement by 360° at operator-set intervals around the unmanned aerial vehicle, with respect to the horizontal axis.

A selected obstacle detection sensor (LiDAR), which is a sensor that measures the direction of the obstacle and the distance thereto, can know a relative position of the obstacle, but cannot measure a velocity of the obstacle. It is determined that velocity information on the obstacle is necessary for avoidance of collision with a mobile obstacle. According to the present invention, the velocity of the obstacle is estimated based on a change in a position of the obstacle. As a filter for estimation, a Kalman filter is used that can predict a state of the obstacle on the basis of the previous state thereof, in a case where the velocity of the obstacle cannot be estimated and the obstacle cannot be measured due to a limitation of the sensor.

The Kalman filter performs two phases, a prediction phase

Date Reçue/Date Received 2020-06-01

and a correction phase. The first phase is a phase in which, for prediction, the next estimation value is computed from a previous estimation value through a system model. The second phase is a phase in which, for correction, the predicted state is corrected by applying data measured in the sensor to the computed estimation value.

In the prediction phase, the next state is predicted from an initial state (x_o) or a correction value (x_k) through the system model (A). Then, a change in Kalman filter error covariance (P_k) due to the prediction of the next state is computed. Equation 1 and Equation 2 are equations that correspond to the prediction phase. x_k^- and P_k^- mean the predicted sate and the error covariance, respectively. w_k and Q mean noise and system nose covariance, respectively, which are generated by the prediction.

Equation 1

$$x_k^- = Ax_{(k-1)} + w_k$$

Equation 2

$$P_k^- = AP_{(k-1)}A^T + Q$$

Date Reçue/Date Received 2020-06-01

where k denotes a step that is used for a Kalman filter variable. A variable of the next step is computed by utilizing a variable of the previous step.

In the correction phase, a Kalman gain (K) is computed from the Kalman filter error covariance and a measurement error covariance (R). A state predicted with a measurement value and the Kalman gain is corrected. Then, the Kalman filter error covariance changed due to the correction is computed. Equations 3 to 5 are equations that correspond to the correction phase. H is a matrix representing a relationship between a measurement value and a state variable.

Equation 3

$$K=P_k^- H^T (HP_k^- H^T+R)^{-1}$$

Equation 4

$$x_k=x_k^-+K(z_k-Hx_k^-)$$

Equation 5

$$P_k=(I-KH)P_k^-$$

According to the present invention, measurement values are an angle with the obstacle and a distance relative thereto, which are obtained from LiDAR. As measurement values, an x-axis distance and a y-axis distance (x_0, y_0) to the obstacle,

Date Reçue/Date Received 2020-06-01

which result from conversion, are used instead of an angle (θ_0) with the obstacle and a distance (d_0) thereto.

Equation 6

$$x_0 = \cos\theta_0 \times d_0$$

Equation 7

$$y_0 = \sin\theta_0 \times d_0$$

In the prediction phase, the next state is estimated from the previous estimation value and the system model, and the changed covariance is estimated while the next state is estimated. In the correction phase, the Kalman gain is computed on the basis of the estimated covariance and a covariance of the measurement value, and the estimated state is corrected on the basis of a difference between a measurement value of the sensor and a prediction value. Then, a pre-correction covariance is again computed.

FIGS. 1A and 1B are a block diagram and a table that show an algorithm of the Kalman filter and constituent elements of the Kalman filter, respectively, according to the present invention.

In order to verify an algorithm for estimating the velocity of the obstacle, which is realized with the Kalman filter, a simulation for detection of the obstacle and estimation of the velocity thereof is realized. The simulation

Date Reçue/Date Received 2020-06-01

is realized in such a manner that performance of the algorithm in terms of LiDAR accuracy and performance of the algorithm in terms of the horizontal-axis LiDAR resolution are comparable. Through the simulation, the performances of the algorithms for estimation of the velocity of the obstacle in terms of LiDAR accuracy and in terms of the horizontal-axis LiDAR resolution were verified. Simulation environments for comparison of the performances of the algorithms in terms of LiDAR accuracy are illustrated as in Table 1.

Table 1

	Case 1	Case 2	Case 3
Simulation time	500 sec	500 sec	500 sec
Step size	0.01 sec	0.01 sec	0.01 sec
Object velocity	about 5 m/s	about 5 m/s	about 5 m/s
LiDAR accuracy	± 3cm	± 10cm	± 20cm
Resolution (Horizontal)	1°	1°	1°

The obstacle moved in the form of a sine wave. The velocity of the obstacle that moved at a velocity of 5 m/s to 5.1 m/s was estimated. The simulation was performed for 500 seconds. LiDAR accuracies were set to 3 cm, 10 cm, and 20 cm, respectively, and LiDAR resolution was set to 1°. Cases 1 to 3

Date Reçue/Date Received 2020-06-01

in each of FIGS. 2 to 4 are results of performing the simulation when the LiDAR accuracies were set to 3 cm, 10 cm, and 20 cm, respectively.

FIG. 2 is a graph comparing an actual value and a measurement value for a path along which the obstacle moves and a result obtained by applying the Kalman filter. FIG. 3 is a graph comparing an actual velocity of the obstacle and a velocity that is estimated with the Kalman filter. FIG. 4 is a graph showing a difference between the actual velocity of the obstacle and the velocity that is estimated with the Kalman filter.

As a result of the simulation, root mean square errors (RMSE) and maximum errors of measurement values and obstacle velocity estimation results are as shown in Table 2.

Date Reçue/Date Received 2020-06-01

Table 2

	Case 1	Case 2	Case 3
Position measurement RMSE	0.0240 m	0.0805 m	0.0805 m
Position measurement maximum error	0.1059 m	0.4098 m	0.6725 m
Position Kalman result RMSE	0.0237 m	0.0797 m	0.6725 m
Position Kalman result maximum error	0.1046 m	0.4062 m	0.6700 m
Velocity Kalman result RMSE	0.0141 m/s	0.0396 m/s	0.0728 m/s
Velocity Kalman result maximum error	0.0595 m/s	0.1632 m/s	0.3759 m/s

As a result of the simulation, RMSEs of LiDAR measurement values in Case 1, Case 2, and Case 3, were 0.0240 m, 0.0805 m, and 0.0805 m, respectively. From this, it can be understood that the greater the LiDAR accuracy, the more RMSE increases. It is shown that RMSEs of estimation velocities of the obstacle are 0.0141 m/s, 0.0396 m/s and 0.0728 m/s, respectively, and that maximum errors of estimation velocities of the obstacle are 0.0595 m/s, 0.1632 m/s, and 0.3759 m/s, respectively. From this, it can be understood that estimations are made with errors of 1.2%, 3.2%, and 7.5%, respectively.

Simulation environments for the comparison of the performances of the algorithms in terms of LiDAR resolution are

Date Reçue/Date Received 2020-06-01

as shown in Table 3.

Table 3

	Case 4	Case 5	Case 6
Simulation time	500 sec	500 sec	500 sec
Step size	0.01 sec	0.01 sec	0.01 sec
Object velocity	about 5 m/s	about 5 m/s	about 5 m/s
LiDAR accuracy	± 3cm	± 3cm	± 3cm
Resolution (Horizontal)	1°	5°	10°

Simulation time and a moving pattern and velocity of an obstacle were set to be the same as those in the previous simulation. A unit expressing the LiDAR accuracy was set to [illegible] cm. The LiDAR resolutions in Cases, 1, 2, and 3 were set to 1°, 5°, and 10°, respectively. Cases 4 to 6 in FIGS. 5 to 7 are the results of the simulation that was performed when the LiDAR resolutions were set to 1°, 5°, and 10°, respectively.

FIG. 5 is a graph comparing the actual value and the measurement value for the path along which the obstacle moves and a result obtained by applying the Kalman filter. FIG. 6 is a graph comparing the actual velocity of the obstacle and the velocity that is estimated with the Kalman filter. FIG. 7 is a

Date Reçue/Date Received 2020-06-01

graph showing the difference between the actual velocity of the obstacle and the velocity that is estimated with the Kalman filter.

As a result of the simulation, root mean square errors (RMSE) and maximum errors of measurement values and obstacle velocity estimation results are as shown in Table 4.

Table 4

	Case 4	Case 5	Case 6
Position measurement RMSE	0.0242m	0.0243m	0.0251m
Position measurement maximum error	0.1140m	0.1040m	0.0971m
Position Kalman result RMSE	0.0240m	0.0240m	0.0248m
Position Kalman result maximum error	0.1129m	0.1035m	0.0964m
Velocity Kalman result RMSE	0.0146m/s	0.0183m/s	0.0250m/s
Velocity Kalman result maximum error	0.0606m/s	0.0553m/s	0.0627m/s

As a result of the simulation, RMSEs of LiDAR measurement values in Case 1, Case 2, and Case 3, were 0.0242 m, 0.0243 m, and 0.0251 m, respectively. From this, it can be understood that a great influence is not exerted on the LiDAR resolutions. RMSEs of estimation velocities of the obstacle are 0.0146 m/s,

Date Reçue/Date Received 2020-06-01

0.0183 m/s, and 0.0250 m/s. From this, it can be understood that the greater the resolution, the more imprecise the velocity estimation of the obstacle. However, the maximum errors of the estimation velocities of the obstacle are 0.0606 m/s, 0.0553 m/s, and 0.0627 m/s, respectively. From this, it can be understood that an error of approximately 1.2% occurs and that the LiDAR resolution does not exert a great influence.

Potential is a scalar field and is computed as a minus gradient of a vector field of a conservative force. A potential field according to the present invention is formed by a force that is generated by a target point and an obstacle in a plane field. An attractive force of the potential field is generated by the target point, and a repulsive force is generated by the obstacle. The potential field is formed by adding up all attractive and repulsive forces. A force that is received by the unmanned aerial vehicle in flight is a result of adding up the attractive force ($\vec{F}_{att}$) and the repulsive force ($\vec{F}_{rep}$) that are generated by all target points and obstacles. A force ($\vec{F}_{total}$) at work that is position-dependent is a force representing a resultant force that results from adding up the attractive force of the target object and the repulsive force of the obstacle.

Date Reçue/Date Received 2020-06-01

Equation 8

$$\vec{F}_{total}(p,v) = \vec{F}_{att}(p,v) + \sum_{i=1}^{n} \vec{F}^{i}_{rep}(p,v)$$

where n denotes the number of detected obstacles. A total repulsive force is computed by adding up repulsive forces of the detected obstacles.

An obstacle avoidance motion by the potential field depends heavily on a component and direction of a force that vary according to a position of the unmanned aerial vehicle. A differential equation of the potential field (U) that varies according to a position and a relative velocity is the same as Equation 9.

Equation 9

$$\vec{\nabla} U(p,v) = \left[\frac{\partial U}{\partial x} \ \frac{\partial U}{\partial y} \right]^{T}$$

A flight trajectory of the unmanned aerial vehicle is formed along the most-steeply-descending direction of the potential field at a current position. This occurs due to a direction of a force at a current position, of the unmanned aerial vehicle, and is regarded as an optimization problem of finding a minimum value of a magnitude of the potential.

According to the present invention, the potential field is configured with an attractive potential field that is generated

Date Reçue/Date Received 2020-06-01

by the target point and represents an attractive force, and a repulsive potential field that is generated by each obstacle and represents a repulsive force.

Generally, the attractive potential field is defined as a function of a relative distance (r_G) between the unmanned aerial vehicle and the target point, and the target point is defined as a point fixed in space. According to the present invention, the attractive potential field is in proportion to the distance (r_G) between the unmanned aerial vehicle and the target point, and a coefficient (K_G) for an attractive force.

Equation 10

$$r_G(p) = \| p_G(t) - p(t) \|$$

$$U_{att} = K_G r_G$$

where $p_G(t)$ and $p(t)$ denote the target point and the position of the unmanned aerial vehicle, respectively, and U_{att} denotes the attractive potential field. An attractive force in the x- and y-directions that is obtained through partial differentiation of the attractive potential field in Equation 10 is summarized as in Equation 11.

Equation 11

Date Reçue/Date Received 2020-06-01

$$F_{att_x} = -\frac{\partial U_{att}}{\partial x} = K_G \frac{(p_{Gx} - p_x)}{r_G}$$

$$F_{att_y} = -\frac{\partial U_{att}}{\partial y} = K_G \frac{(p_{Gy} - p_y)}{r_G}$$

Equation 12

$$e_{Gx} = \frac{p_{Gx} - p_x}{r_G}, \quad e_{Gy} = \frac{p_{Gy} - p_y}{r_G}$$

Equation 13

$$F_{att_x} = K_G e_{Gx}, \quad F_{att_y} = K_G e_{Gy}$$

e_{Gx} and e_{Gy} in Equation 12 denote the respective directions of the unmanned aerial vehicle and the target point as unit vector components. For expression in terms of a unit vector, Equation 11 is summarized as the product of a unit vector and the coefficient of the attractive force as Equation 13. Therefore, a magnitude of the attractive force is fixed regardless of a distance between the unmanned aerial vehicle and the target point, and it can be understood that the attractive force also has a fixed influence regardless of the position of the unmanned aerial vehicle.

A general repulsive potential field is defined as a function of a distance between the unmanned aerial vehicle and the obstacle. However, in a downtown area, it is necessary to

Date Reçue/Date Received 2020-06-01

avoid collision not only with a stationary obstacle, but also with a moving obstacle, such as a vehicle, a bird, and another unmanned aerial vehicle. When the repulsive potential field is defined only as the function of the distance, the velocity of the obstacle is not taken into consideration, thereby increasing the risk of collision. According to the present invention, the collision with obstacles, including a moving obstacle and a stationary obstacle, is avoidable by applying not only the distance between the unmanned aerial vehicle and the obstacle, but also the relative velocity.

The repulsive potential field according to the present invention is generated by utilizing the distance between the unmanned aerial vehicle and the obstacle, the relative velocity, and the like. An equation for applying the distance (r_O) to the obstacle and the relative velocity (v_{RO}) is the same as Equation 14.

Equation 14

$$v_{RO}(t)=[v(t)-v_O(t)]^T n_{RO}$$

$$r_O(p(t), p_{O(t)})=\| p(t)-p_O(t) \|$$

where v, v_O denotes the respective velocities of the unmanned aerial vehicle and the obstacle and p_O denotes a position of the obstacle. In addition, n_{RO} denotes a direction

Date Reçue/Date Received 2020-06-01

of a v_{RO} vector. In order to efficiently avoid collision of the unmanned aerial vehicle, a braking distance (r_m) of the unmanned aerial vehicle and an influence range (r_s) of the obstacle are applied. The influence range of the obstacle may vary according to an operating environment. Generally, an operator sets the influence range of the obstacle in such a manner as to have a value suitable for the operating environment.

The repulsive potential field that results from applying the braking distance of the unmanned aerial vehicle and the influence range of the obstacle is as in Equation 15. In a case where the unmanned aerial vehicle falls out of the influence range of the obstacle, or in a case where the distance to the obstacle is constant or increases, the repulsive potential field is not generated. In a case where the distance to the obstacle increases, but falls within the influence range of the obstacle, the repulsive potential field is not defined.

Equation 15

$$r_m = \frac{v_{RO}^2(t)}{2a_{\max}}$$

Equation 16

Date Reçue/Date Received 2020-06-01

$$U_{rep}(p,v) = \begin{cases} 0, & \text{if } r_O - r_m \geq r_s \text{ or } v_{RO} \leq 0 \\ K_O\left(\frac{1}{r_O - r_m} - \frac{1}{r_s}\right) & \text{if } 0 < r_O - r_m < r_s \text{ and } v_{RO} > 0 \\ not\,defined & v_{RO} < 0 \text{ and } r_O - r_m < r_s \end{cases}$$

a_{max} in Equation 15 denotes maximum acceleration of the unmanned aerial vehicle. K_O In Equation 16 denotes a coefficient of a repulsive force. Application of a general potential field to the unmanned aerial vehicle makes it necessary to adjust the coefficient of the repulsive force according to a change in the velocity of the unmanned aerial vehicle. According to the present invention, the relative velocity of the unmanned aerial vehicle with respect to the obstacle is applied. Thus, the potential field changes when the velocity of the unmanned aerial vehicle changes. Therefore, the velocity of the unmanned aerial vehicle is changeable during the flight of the unmanned aerial vehicle.

Like the attractive force, the repulsive force is obtained through the differentiation of the repulsive potential field, and it can be summarized as in Equation 17. In the case where the unmanned aerial vehicle falls out of the influence range of the obstacle or in the case where the distance to the obstacle is constant or increases, the repulsive force is not generated. In the case where the distance to the obstacle increases but

Date Reçue/Date Received 2020-06-01

falls within the influence range of the obstacle, the repulsive force is not defined.

Equation 17

$$F_{rep}(p,v) = \begin{cases} 0, & \text{if } r_O - r_m \geq r_s \text{ or } v_{RO} \leq 0 \\ F_{rep1} + F_{rep2} & \text{if } 0 < r_O - r_m < r_s \text{ and } v_{RO} > 0 \\ not\,defined & v_{RO} < 0 \text{ and } r_O - r_m < r_s \end{cases}$$

$$F_{rep1} = K_O U_{rep}^2 (1 + \frac{v_{RO}(t)}{a_{max}}) n_{OR}$$

$$F_{rep2} = \frac{K_O U_{rep}^2 v_{RO}(t) v_{RO\perp}}{a_{max} r_O(p(t), p_O(t))} n_{OR\perp}$$

where F_{rep1} denotes a repulsive force that is generated, in the direction of the obstacle, in the unmanned aerial vehicle, F_{rep2} denotes a repulsive force that is generated in a direction vertical to F_{rep1}, $v_{RO\perp}$ is a component in the vertical direction, of a v_{RO} vector, $n_{RO\perp}$ is a component in the vertical direction, of a v_{RO} vector and n_{OR} is a reverse vector of n_{RO}.

FIGS. 14 and 15 illustrate the respective examples, respectively, of the repulsive potential field and a repulsive

Date Reçue/Date Received 2020-06-01

potential field contour that result when it is assumed that there is no motion of the obstacle. Coordinates of the obstacle are (3, 3), (8, 6), and (8, 9).

A local minimum in analytics means a function value at a minimum point. That is, various local minimums may be present, as function values that are minimized at all points in the vicinity, in a high-order function.

The collision avoidance algorithm based on the potential field is an algorithm for avoiding the obstacle while moving in a gradient descent direction of a potential force. The collision avoidance based on the potential field may lead to the local minima phenomenon where a minimum value of the potential field is reached locally before reaching a target point. In this potential field, there are three types of situations where a minimum value occurs locally instead of occurring at a final target point.

First, in a case where the unmanned aerial vehicle, the obstacle, and the target point are on the same line and where the obstacle is positioned between the unmanned aerial vehicle and the target point, the local minima phenomenon may occur. In such a case, when the attractive force and the repulsive force are the same, the unmanned aerial vehicle can hover at a fixed position without moving to the target point. FIG. 16 illustrates in the first local minima.

Second, in a case where the unmanned aerial vehicle moves

Date Reçue/Date Received 2020-06-01

toward the target point and obstacles are positioned to the left and right, respectively, of a moving path, the local minima phenomenon may also occur. When the repulsive force that is generated by the respective obstacles on the left and right of the path to the target point and the attractive force that is generated by the target point are balanced, the unmanned aerial vehicle may not move to the target point. FIG. 17 illustrates the second local minima.

Third, in a case where the target point is positioned within the range where the obstacle exerts an influence and where the repulsive force generated by the obstacle is greater than the attractive force generated by the target point, the local minima phenomenon where the unmanned aerial vehicle cannot reach the target point may occur. FIG. 18 illustrates the third local minima.

When the attractive force generated by the target point and the repulsive force generated by the obstacle are balanced, the local minima phenomenon occurs. Therefore, in an environment where obstacles are present, such as in a downtown area, there is a high likelihood that the local minima phenomenon will occur.

According to the present invention, in a case where an amount of change in the position of the unmanned aerial vehicle is below a threshold, it is determined that the local minima phenomenon occurs. Then, an attempt was made to overcome the

Date Reçue/Date Received 2020-06-01

local minima by changing the coefficient of the repulsive force. d in FIG. 19 denotes a distance the unmanned aerial vehicle moves for a fixed time, and α denotes the time for determining the local minima. K_0 denotes a coefficient of the repulsive force. s is a variable for setting an amount of change in the coefficient of the repulsive force in a case where it is determined that the local minima occurs. According to the present invention, s is set to a number that is greater than 1 in such a manner that the coefficient of the repulsive force is reduced in a case where an amount of motion is small.

The collision avoidance algorithm based on the potential field uses a method in which the collision with the obstacle is avoided by moving in the direction of the potential force computed through the differentiation of the potential field.

As in Equation 10, the attractive potential field that is used for the collision avoidance algorithm is generated in proportion to the distance between the unmanned aerial vehicle and the target point. As in Equation 16, the repulsive potential field is generated by reflecting not only the distance between the unmanned aerial vehicle and the obstacle but also the relative velocity. The respective characteristics of the unmanned aerial vehicle and the obstacle are reflected

Date Reçue/Date Received 2020-06-01

by utilizing parameters such as the braking distance and the influence of the obstacle. The potential force is obtained by differentiating the sum of the generated attractive potential field and repulsive potential field, and the obtained potential force is utilized for guided navigation of the unmanned aerial vehicle. An equation for the potential force and an equation for heading control of the unmanned aerial vehicle in the direction of the potential force are the same as Equations 18 to 20.

Equation 18

$$F_x = F_{attx} + F_{1repx} + F_{2repx} + \cdot \cdot \cdot + F_{nrepx}$$

$$F_y = F_{atty} + F_{1repy} + F_{2repy} + \cdot \cdot \cdot + F_{nrepy}$$

Equation 19

$$\psi_{CMD} = \tan^{-1}\left(\frac{F_y}{F_x}\right)$$

Equation 20

$$\beta = K_C(\psi_{CMD} - \psi)$$

In Equation 20, K_C denotes a control coefficient, and β denotes a direction control value of the unmanned aerial vehicle. FIG. 20 is a flowchart for the collision avoidance algorithm based on the potential field. The potential forces in the horizontal and vertical axes, which are generated by the

Date Reçue/Date Received 2020-06-01

potential field, are computed based on a current position and a target point that are measured and set, respectively, in the unmanned aerial vehicle and information on the obstacle measured in LiDAR. The direction of the potential force is computed using an arctangent in the potential forces in the horizontal and vertical axes, and a heading command of the unmanned aerial vehicle is determined in the direction of the potential force. The heading of the unmanned aerial vehicle is controlled with a value that results from multiplying a heading error of the unmanned aerial vehicle by a heading control coefficient. FIG. 20 illustrates a collision avoidance algorithm according to the present invention.

The embodiment of the present invention is described only in an exemplary manner referring to the drawings. It will be apparent to a person of ordinary skill in the art to which the present invention pertains that various other modifications and equivalents are possible from this description.

Date Reçue/Date Received 2020-06-01

WHAT IS CLAIMED IS:

1. A method of avoiding collision of an unmanned aerial vehicle with an obstacle, the method comprising:

calculating two potential fields using current positional information of the unmanned aerial vehicle, a target point that is set, and positional information of the obstacle measured by a sensor;

computing an attractive force and a repulsive force by differentiating the computed potential fields, respectively;

computing a direction of a potential force that results from adding up the computed attractive force and repulsive force; and

performing control that brings about a change from the computed direction of the potential force to a direction in which the unmanned aerial vehicle moves;

wherein the step of computing of the potential field includes an attractive potential field that is computed with the current positional information of the unmanned aerial vehicle and the target point that is set, and a repulsive potential field that is computed with the current positional information of the unmanned aerial vehicle and a positional information of the obstacle,

the repulsive potential field is proportional to a coefficient of the repulsive force that is a set coefficient,

a change in the position of the unmanned aerial vehicle for a set time is computed,

the coefficient of the repulsive force is reduced in a case where the computed change in the position of the unmanned aerial vehicle is smaller than a setting value, and

the case where the computed change in the position of the unmanned aerial vehicle is smaller than the setting value for

Date Reçue/Date Received 2022-10-05

the given time is a case where the target point is positioned within a range where the obstacle exerts an influence and the repulsive force that is generated by the obstacle is greater than the attractive force that is generated by the target point.

2. The method according to claim 1, wherein in the step of computing of the potential field the potential fields include: an attractive potential field that is computed with the current positional information of the unmanned aerial vehicle and the target point that is set, and a repulsive potential field that is computed with the current positional information of the unmanned aerial vehicle and a positional information of the obstacle, and

the attractive potential field is computed using the following equation:

Equation

$$r_G(p) = \| p_G(t) - p(t) \|$$

$$U_{att} = K_G r_G$$

where r_G denotes a distance between the unmanned aerial vehicle and the target point, K_G denotes a coefficient of the attractive force, $p_G(t)$ denotes the target point, $p(t)$ denotes a position of the unmanned aerial vehicle, and U_{att} denotes the attractive potential field.

3. The method according to claim 2, wherein an attractive force is computed from the attractive potential field, and

the attractive force is computed using the following equations:

Date Reçue/Date Received 2022-10-05

Equation

$$F_{att\,x} = -\frac{\partial U_{att}}{\partial x} = K_G \frac{(p_{Gx} - p_x)}{r_G}$$

$$F_{att\,y} = -\frac{\partial U_{att}}{\partial y} = K_G \frac{(p_{Gy} - p_y)}{r_G}$$

.

4. The method according to claim 3, wherein the repulsive potential field is computed using the following equations:

Equation

$$U_{rep}(p,v) = \begin{cases} 0, & \text{if } r_O - r_m \geq r_s \text{ and } v_{RO} \leq 0 \\ K_O\left(\frac{1}{r_O - r_m} - \frac{1}{r_s}\right) & \text{if } 0 < r_O - r_m < r_s \text{ and } v_{RO} > 0 \\ \text{not defined} & \text{if } r_O - r_m < r_s \text{ and } v_{RO} < 0 \end{cases}$$

where r_O denotes a distance between the unmanned aerial vehicle and the obstacle, and v_{RO} denotes the respective relative velocities of the unmanned aerial vehicle and the obstacle;

Equation

$$v_{RO}(t) = [v(t) - v_O(t)]^T n_{RO}$$

$$r_O(p(t), p_O(t)) = \| p(t) - p_O(t) \|$$

where v denotes a velocity of the unmanned aerial vehicle, v_O denotes a velocity of the obstacle, p_O denotes a position of the obstacle, r_m denotes a braking distance of the unmanned

Date Reçue/Date Received 2022-10-05

aerial vehicle, and r_s denotes an influence range of the obstacle; and

$$r_m = \frac{v_{RO}^2(t)}{2a_{max}}$$

where a_{max} denotes maximum acceleration of the unmanned aerial vehicle, K_O denotes a coefficient of the repulsive force, and n_{RO} denotes a direction of a v_{RO} vector.

5. The method according to claim 4, wherein a repulsive force is computed from the repulsive potential field, and

the repulsive force is computed using the following equations:

Equation

$$F_{rep}(p,v) = \begin{cases} 0, & \text{if } r_O - r_m \geq r_s \text{ and } v_{RO} \leq 0 \\ F_{rep1} + F_{rep2} & \text{if } 0 < r_O - r_m < r_s \text{ and } v_{RO} > 0 \\ not\,defined & \text{if } r_O - r_m < r_s \text{ and } v_{RO} < 0 \end{cases}$$

$$F_{rep1} = K_O U_{rep}^2 \left(1 + \frac{v_{RO}(t)}{a_{max}}\right) n_{OR}$$

$$F_{rep2} = \frac{K_O U_{rep}^2 v_{RO}(t) v_{RO\perp}}{a_{max} r_O(p(t), p_O(t))} n_{OR\perp}$$

where F_{rep1} denotes a repulsive force that is generated, in a direction of the obstacle, in the unmanned aerial vehicle,

Date Reçue/Date Received 2022-10-05

F_{rep2} denotes a repulsive force that is generated in a direction vertical to F_{rep1}, $v_{RO\perp}$ denotes a magnitude in a vertical direction, of a v_{RO} vector, $n_{RO\perp}$ denotes a component in a vertical direction, of a v_{RO} vector and n_{OR} is a reverse vector of n_{RO}.

Date Reçue/Date Received 2022-10-05

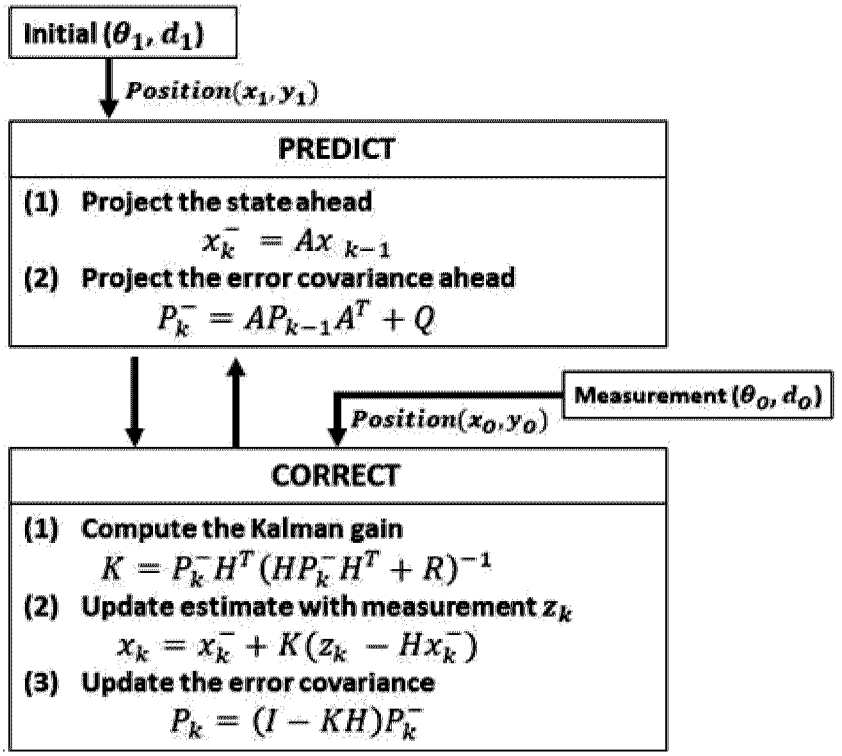

FIG. 1a

Date Reçue/Date Received 2020-06-01

● State transition	$A=\begin{bmatrix}1 & 0 & \Delta t & 0\\ 0 & 1 & 0 & \Delta t\\ 0 & 0 & 1 & 0\\ 0 & 0 & 0 & 1\end{bmatrix}$
● Kalman error covariance	$P=I_4$
● Process noise covariance	$Q=\begin{bmatrix}1 & 0 & 0 & 0\\ 0 & 1 & 0 & 0\\ 0 & 0 & 5 & 0\\ 0 & 0 & 0 & 5\end{bmatrix}$
● Measurement state transition	$H=\begin{bmatrix}1 & 0 & 0 & 0\\ 0 & 1 & 0 & 0\end{bmatrix}$
● Measurement noise covariance	$R=\begin{bmatrix}0.01 & 0\\ 0 & 0.01\end{bmatrix}$
● Measurement Matrix	$z_k=[x_O \;\; y_O]^T$

FIG. 1b

Date Reçue/Date Received 2020-06-01

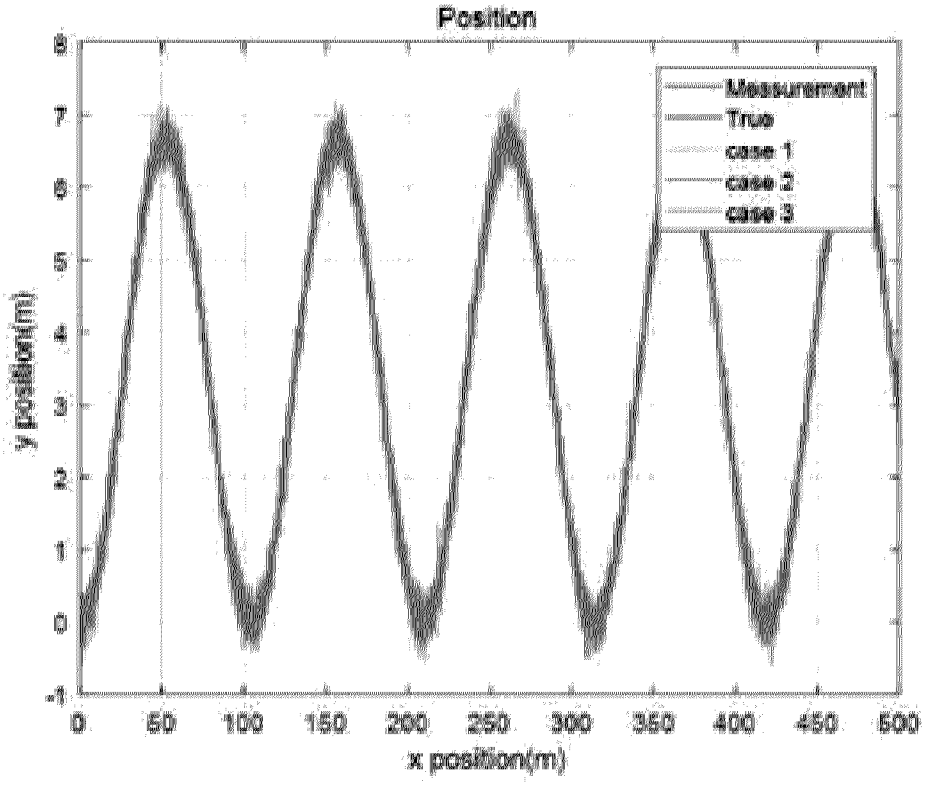

FIG. 2

Date Reçue/Date Received 2020-06-01

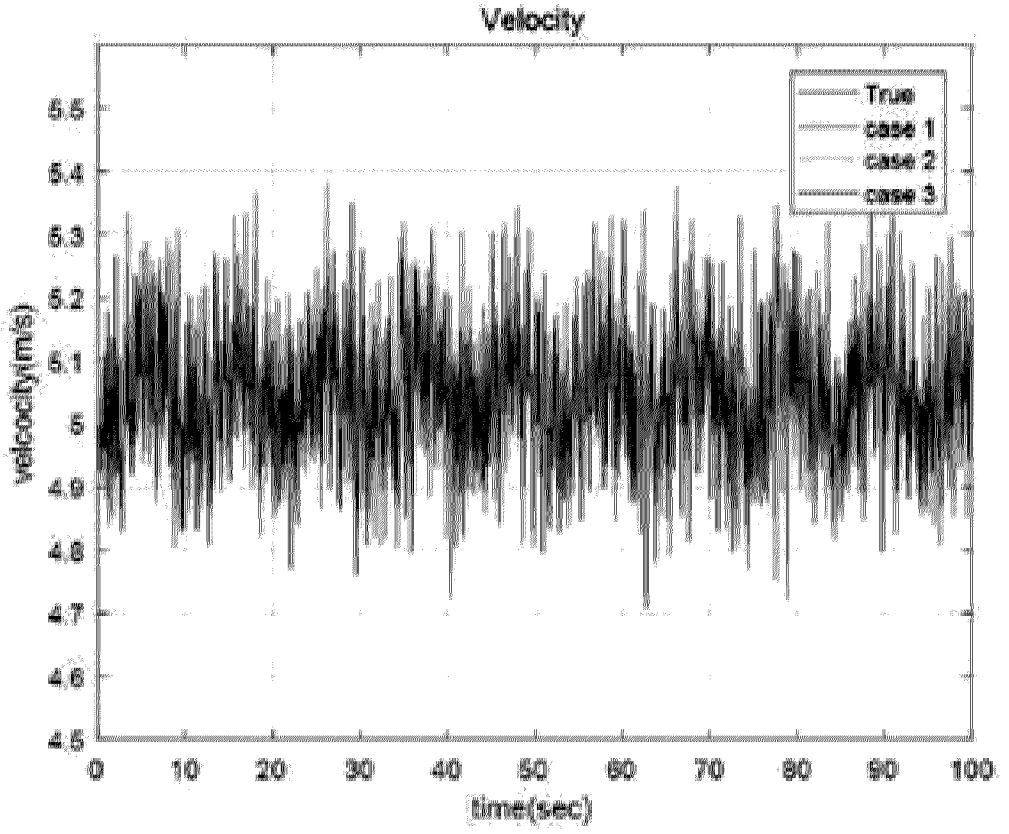

FIG. 3

Date Reçue/Date Received 2020-06-01

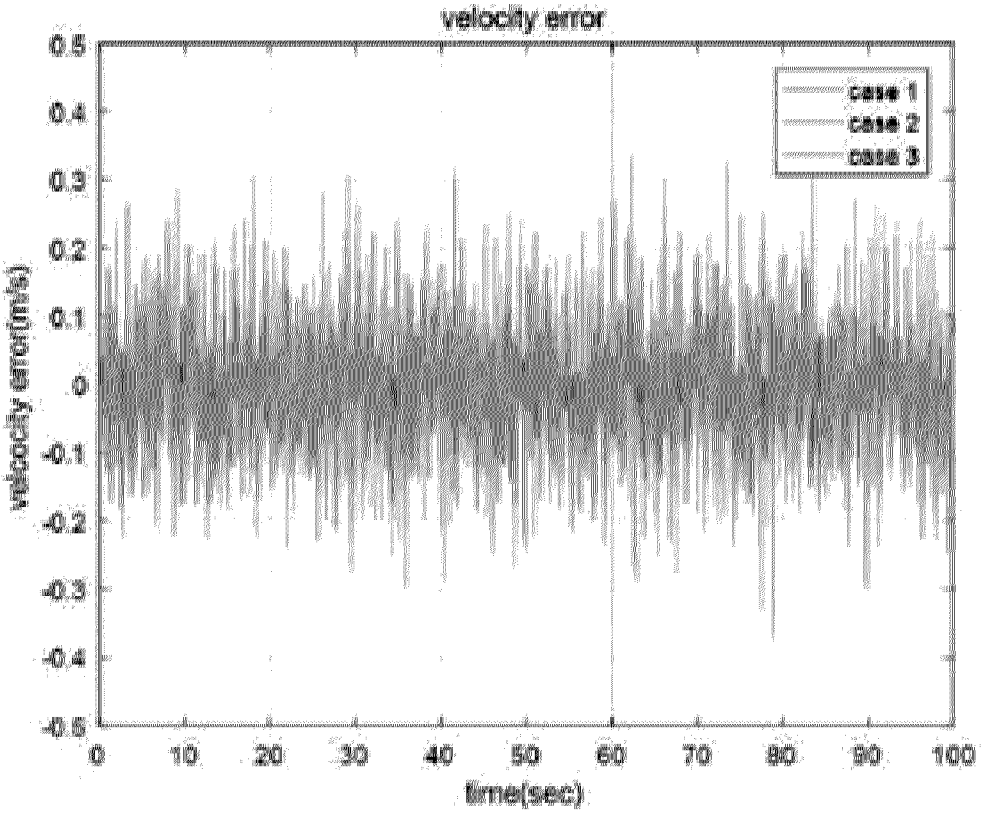

FIG. 4

Date Reçue/Date Received 2020-06-01

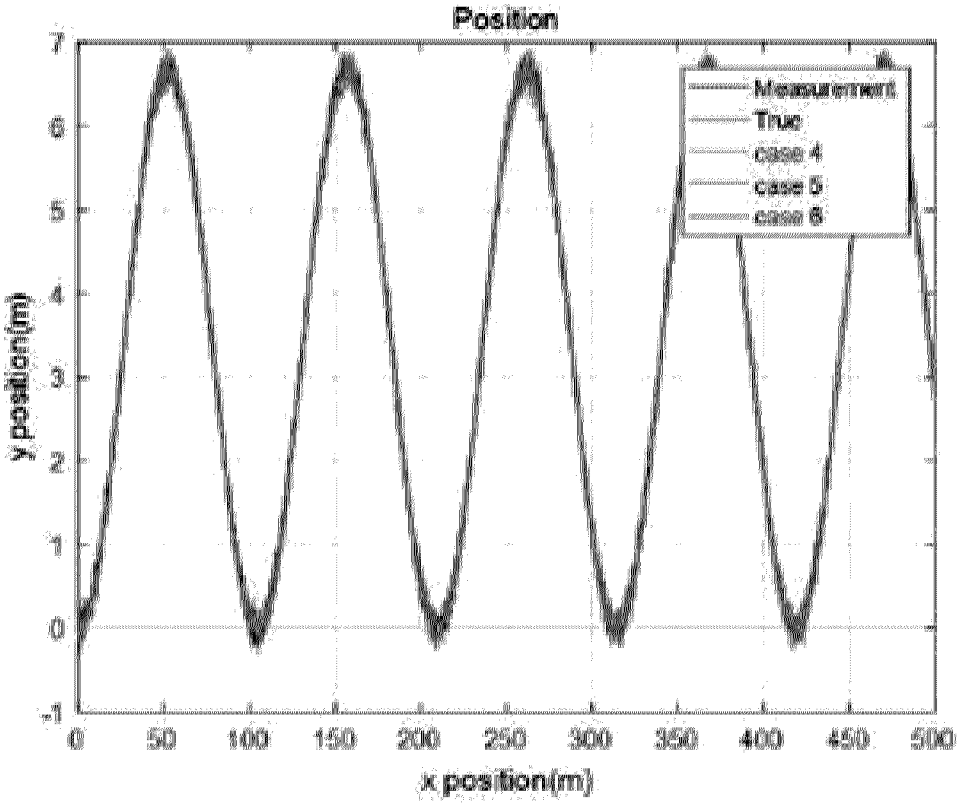

FIG. 5

Date Reçue/Date Received 2020-06-01

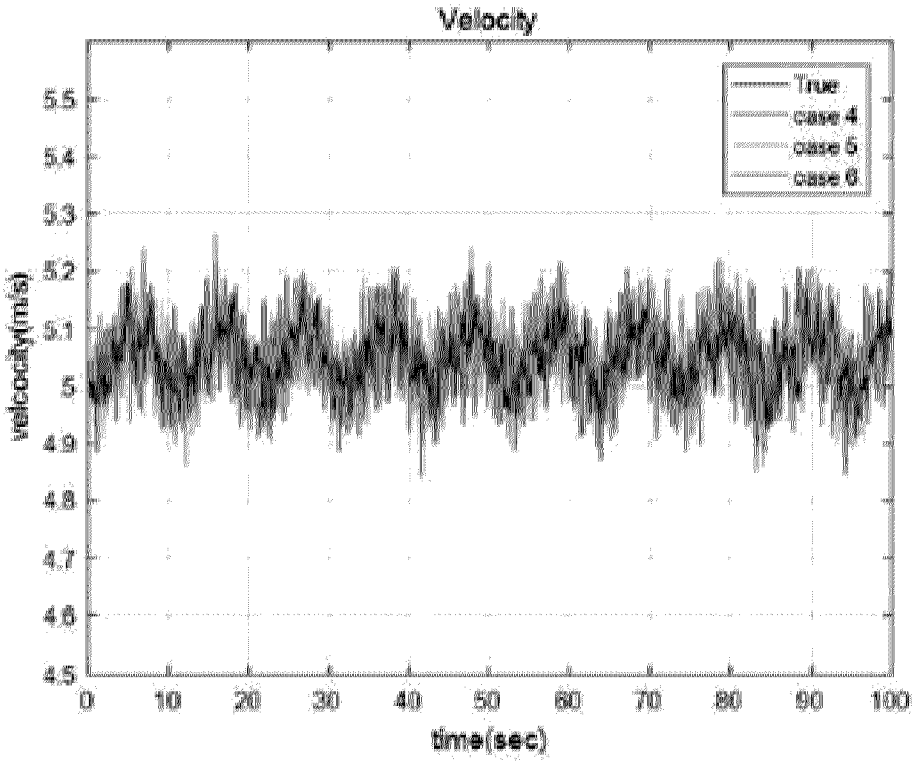

FIG. 6

Date Reçue/Date Received 2020-06-01

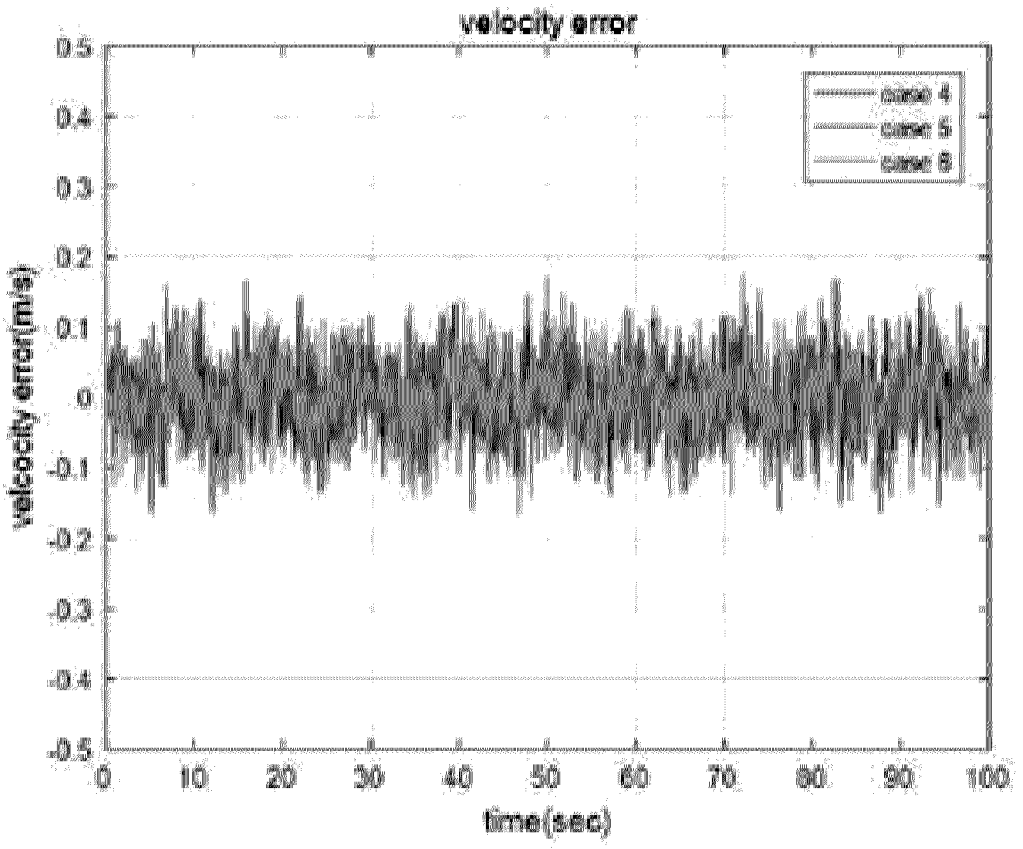

FIG. 7

Date Reçue/Date Received 2020-06-01

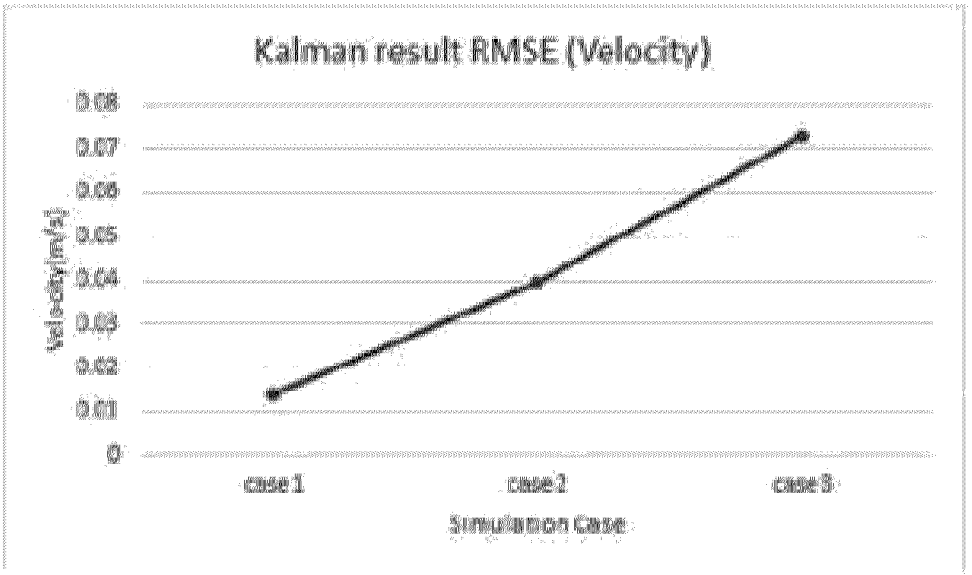

FIG. 8

Date Reçue/Date Received 2020-06-01

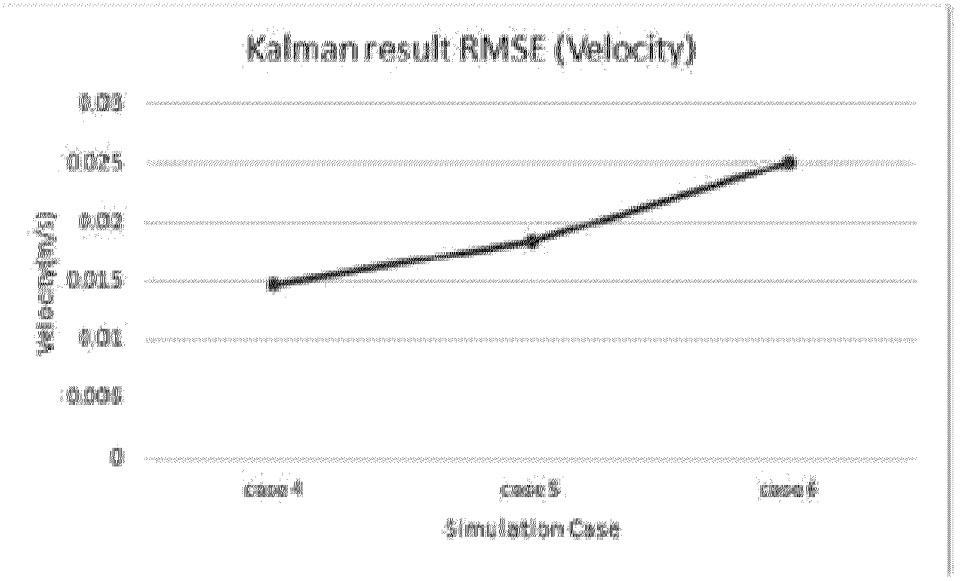

FIG. 9

Date Reçue/Date Received 2020-06-01

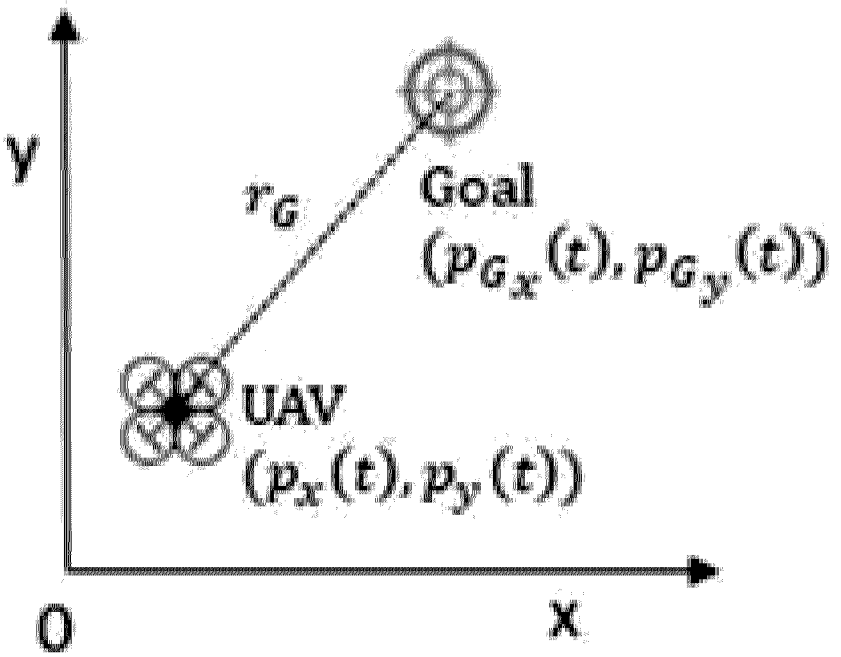

FIG. 10

Date Reçue/Date Received 2020-06-01

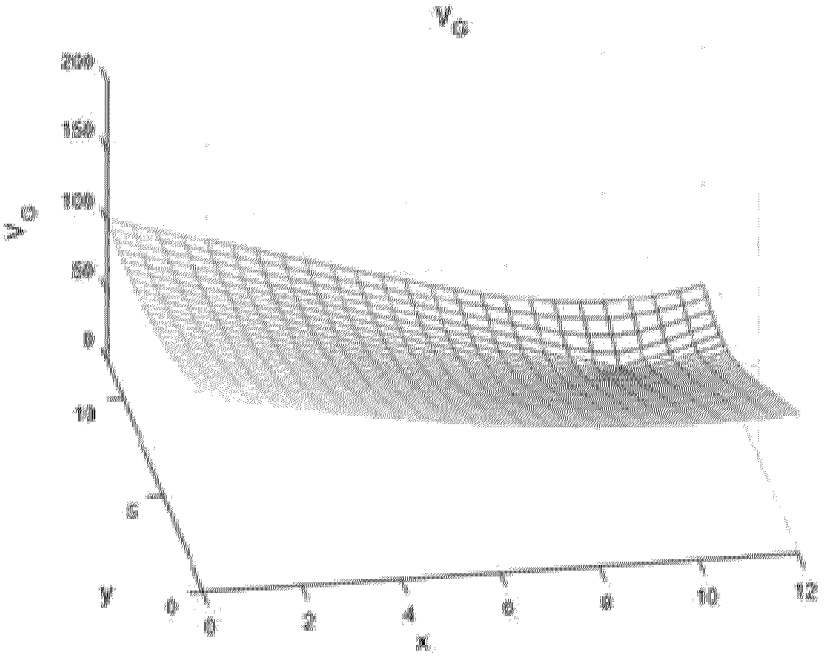

FIG. 11

Date Reçue/Date Received 2020-06-01

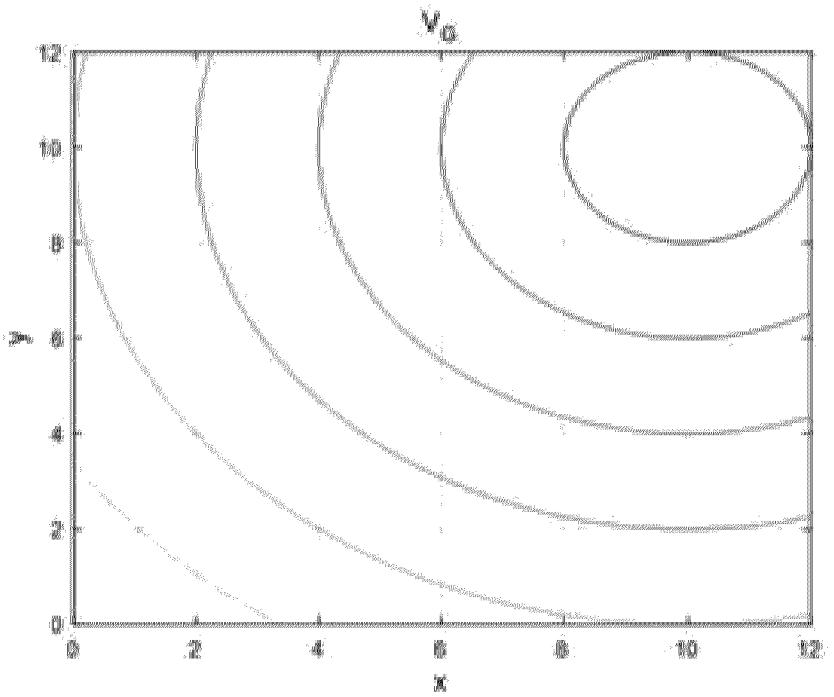

FIG. 12

Date Reçue/Date Received 2020-06-01

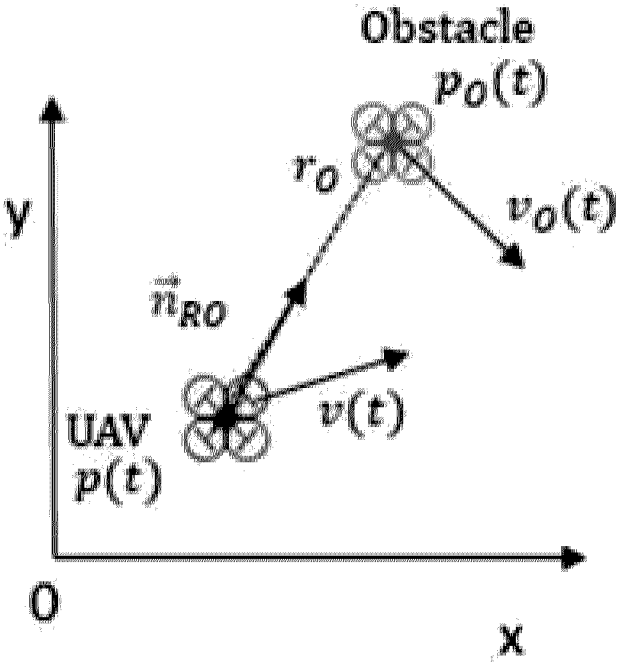

FIG. 13

Date Reçue/Date Received 2020-06-01

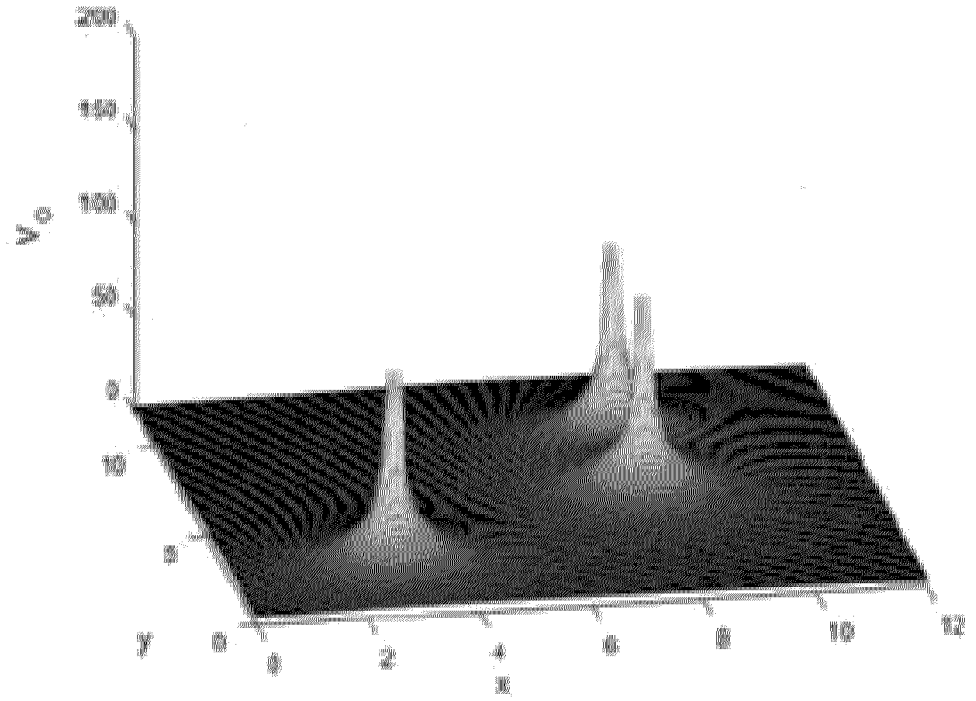

FIG. 14

Date Reçue/Date Received 2020-06-01

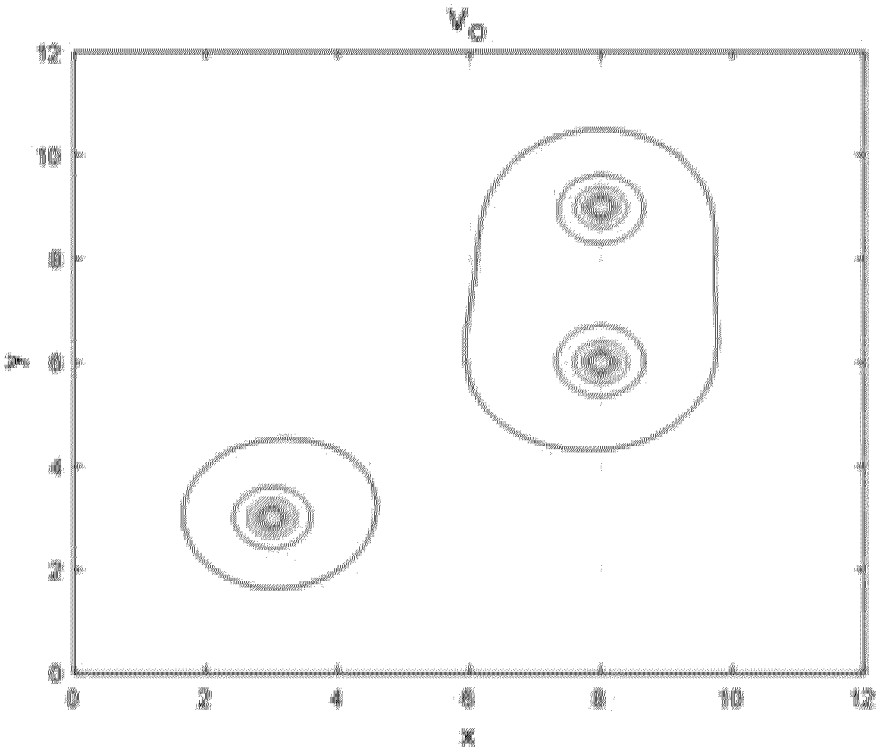

FIG. 15

Date Reçue/Date Received 2020-06-01

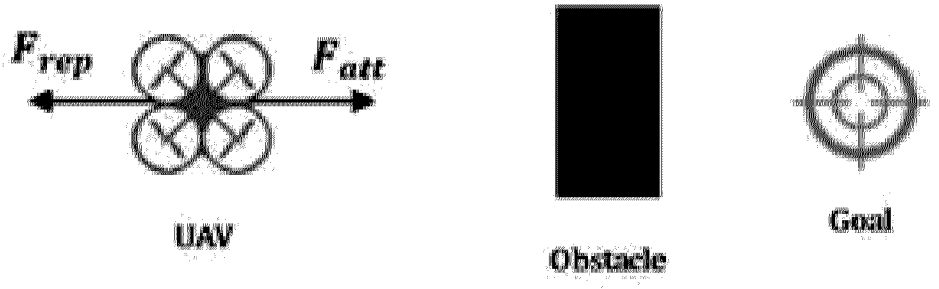

FIG. 16

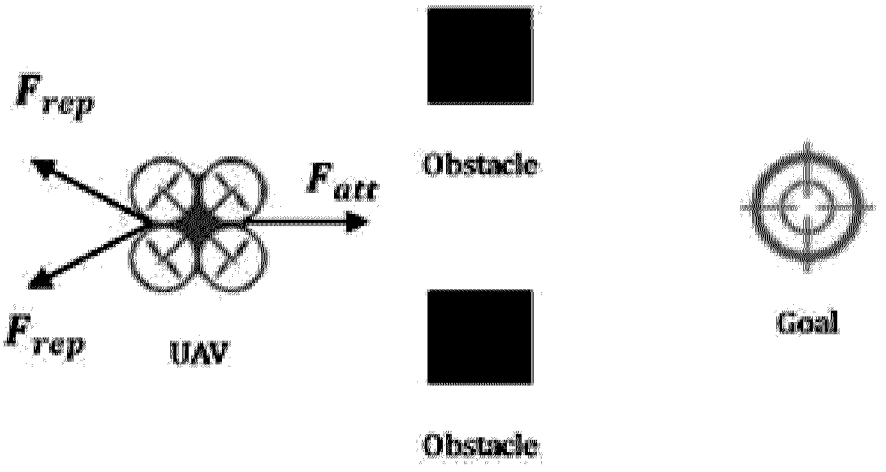

FIG. 17

Date Reçue/Date Received 2020-06-01

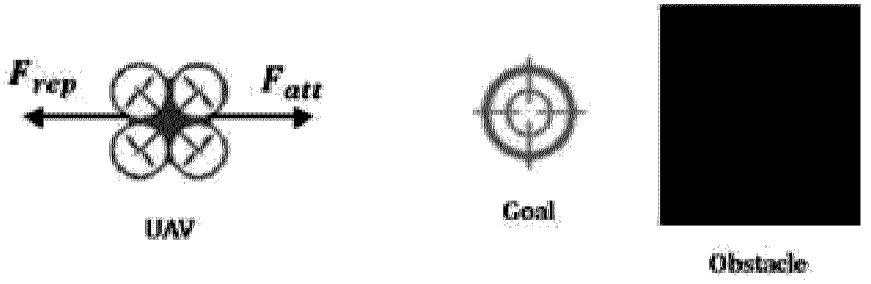

FIG. 18

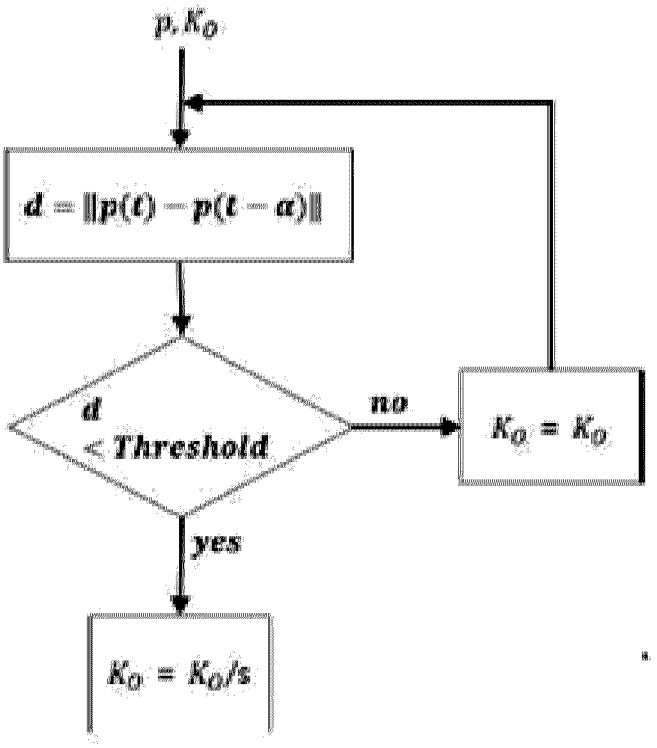

FIG. 19

Date Reçue/Date Received 2020-06-01

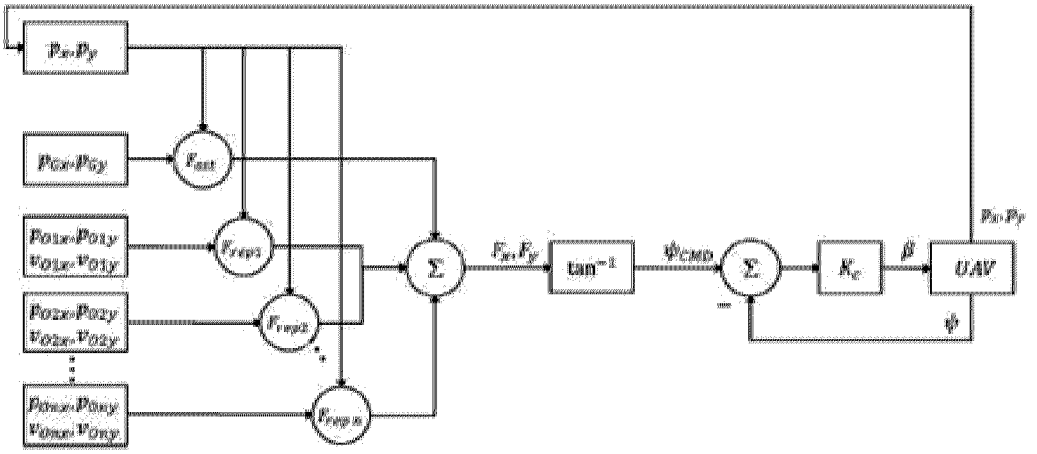

FIG. 20

Date Reçue/Date Received 2020-06-01

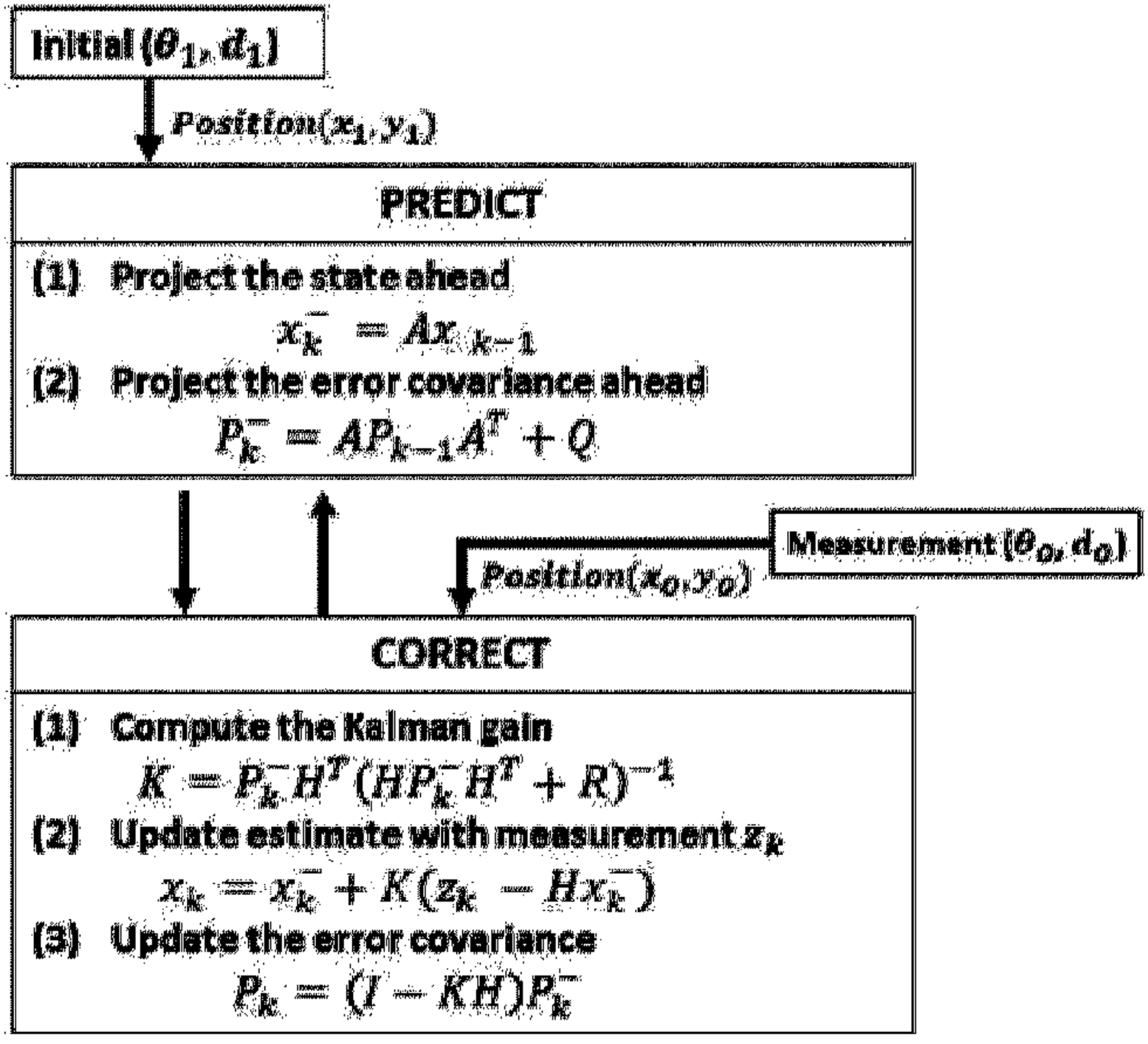
Initial (θ_1, d_1)
$Position(x_1, y_1)$
PREDICT
(1) Project the state ahead
$\bar{x}_k = Ax_{k-1}$
(2) Project the error covariance ahead
$P_k^- = AP_{k-1}A^T + Q$
Measurement (θ_0, d_0)
$Position(x_0, y_0)$
CORRECT
(1) Compute the Kalman gain
$K = P_k^- H^T (HP_k^- H^T + R)^{-1}$
(2) Update estimate with measurement z_k
$x_k = \bar{x}_k + K(z_k - H\bar{x}_k)$
(3) Update the error covariance
$P_k = (I - KH)P_k^-$